

## SYNAPTIC HYPERPOLARIZATION AND INHIBITION OF TURTLE COCHLEAR HAIR CELLS

By J. J. ART, R. FETTIPLACE AND P. A. FUCHS\*

*From the Physiological Laboratory, University of Cambridge, Cambridge CB2 3EG*

*(Received 4 November 1983)*

### SUMMARY

1. Intracellular recordings were made from turtle cochlear hair cells in order to examine the properties of the post-synaptic potentials evoked by electrical stimulation of the efferent axons.

2. Single shocks to the efferents generated a hair cell membrane hyperpolarization with an average amplitude generally less than 1 mV and lasting for about 100 ms. With short trains of shocks, the size of the post-synaptic potential grew markedly to a maximum of 20–30 mV.

3. The interaction between pairs of shocks separated by a varying interval was studied. For an interval of 4 ms, the response to the second shock was increased on average by a factor of 3 and the conditioning effect of the first shock decayed with a time constant of about 100 ms. We suggest the augmentation in response to trains of shocks may be partly due to facilitation of efferent transmitter release.

4. The efferent post-synaptic potentials could be reversibly abolished by perfusion with perilymphs containing 3  $\mu$ M-curare or atropine, and infusion of acetylcholine gave a transient membrane hyperpolarization. These observations are consistent with efferent action being mediated via a cholinergic synapse onto the hair cells.

5. The post-synaptic potentials could be reversed in polarity by injection of hyperpolarizing currents through the recording electrode. The reversal potential was estimated as about  $-80$  mV, 30 mV negative to the resting potential. Near reversal, a small brief depolarization was evident and may constitute a minor component of the synaptic response.

6. The value of the reversal potential was unaffected by substitution of the perilymphatic chloride, but was altered in a predictable manner by changes in extracellular potassium concentration indicating that the post-synaptic potentials arise mainly by an increase in the permeability of the hair cell membrane to potassium ions.

7. Throughout the post-synaptic hyperpolarization there was a reduction in the sensitivity of the hair cell to tones at its characteristic frequency. The desensitization, maximal for low sound pressures, varied in different cells from a factor of 1.6 to 28. At the peak of the largest synaptic potentials, the receptor potential remained negative to the resting potential with all but the loudest characteristic frequency tones.

8. We suggest that there are two factors in efferent inhibition: one a reduction in

\* Present address: Department of Physiology, University of Colorado School of Medicine, 4200 East Ninth Avenue, Denver, CO 80262, U.S.A.

the receptor potential at the hair cell's characteristic frequency and the other a hyperpolarization of its membrane potential which should reduce the release of excitatory transmitter onto the afferent terminals. On the assumption that a hair cell receptor potential of about 1.0 mV causes a threshold response in an auditory afferent fibre (Crawford & Fettiplace, 1980) then a maximum threshold elevation of 60–80 dB in the afferents can be accounted for by efferent action on the hair cells.

9. Intracellular recordings from afferent nerve terminals showed that during efferent stimulation, there was a cessation of all driven activity with no change in the membrane potential.

#### INTRODUCTION

Although there have been many studies on the cochlear efferent system (Klinke & Galley, 1974), no information is available to relate the efferent effects on their targets, the sensory hair cells, to inhibition of the cochlear output. Hyperpolarizing post-synaptic potentials, produced by efferent axonal stimulation, have been recorded in hair cells of the saccule (Ashmore & Russell, 1982) and the lateral line organ (Flock & Russell, 1976), where it was suggested that they would regulate transmitter release at the afferent synapse, but the idea was not tested quantitatively. In the preceding paper efferent inhibition was characterized in the turtle cochlea by recording the responses of auditory nerve afferents (Art & Fettiplace, 1984). Efferent action was shown to display a number of distinctive features including (i) a potent desensitization graded over four orders of magnitude to reflect the maximal range of sound intensities to which the animal might be exposed, (ii) an enhancement of inhibition with each successive efferent stimulus in a train, (iii) a modification of the cochlea's frequency selectivity, manifested as a reduction in the sharpness of tuning of individual afferents. The origin of these properties, which can most properly be examined by recording the inhibitory post-synaptic potentials (i.p.s.p.s) in single hair cells, is the subject of the work to be presented. Here we shall describe the factors responsible for the magnitude of the efferent effect, and show that the inhibition of the afferent fibre responses can be largely understood in terms of the changes in membrane potential and conductance of the hair cells. The efferent interaction with the hair cell's tuning process will be deferred until a later paper (J. J. Art, A. C. Crawford, R. Fettiplace & P. A. Fuchs, unpublished). Some aspects of these results have been published in a preliminary form (Art, Crawford, Fettiplace & Fuchs, 1982, 1983).

#### METHODS

##### *Preparation and recording techniques*

The techniques for intracellular recording from single hair cells in isolated half-heads of adult red-eared turtles *Pseudemys scripta elegans* (carapace length 70–150 mm) were similar to those used in earlier experiments (Crawford & Fettiplace, 1980, 1981*a*). A detailed account of the preparation and methods for stimulating the efferent axons is presented in the preceding paper (Art & Fettiplace, 1984). Briefly, after decapitation of the turtle, the head was split in the mid line, most of the brain removed and the scala tympani opened from the cranial side. For experiments in which the scala tympani was perfused, the aperture in the otic capsule was extended posteriorly to the

metotic fissure. The tympanum was sealed to an acoustic coupler connected to an earphone (Beyer DT48) and monitoring microphone, and the preparation was mounted in a chamber gassed with a moist 95% O<sub>2</sub>:5% CO<sub>2</sub> mixture. The efferent axons were stimulated with trains of constant current pulses (0.4 ms duration, 20–300  $\mu$ A) delivered by platinum electrodes at the junction between the two roots of the VIIIth nerve where they exit from the residual piece of medulla. Unless otherwise indicated, the repetition rate for the trains of efferent shocks was 2/s and the intershock interval was 4 ms. All experiments were performed with the preparation inside a double-walled Industrial Acoustics 1202A sound attenuating chamber.

Glass micropipettes drawn on a Brown-Flaming puller and filled with 4 m-potassium acetate plus 0.1 m-potassium chloride (resistances 200–500 M $\Omega$ ) were advanced into the basilar papilla from the scala tympani, so penetrating the bases of the hair cells. Intracellular potentials were measured with respect to a chloridized silver wire inserted into the cervical spinal cord, which served as a tissue bridge and was in fluid continuity with the scala tympani. The recording electrode was connected to a high input impedance amplifier with capacity compensation and the facility for constant current injection. When currents (up to 0.6 nA) were injected down the recording electrode in order to polarize the hair cell, the discontinuity on the rising phase of the voltage response was used as an indication of the potential drop across the electrode resistance; this potential was balanced out either during an experiment or at the later stage of data analysis, applying the same criterion to averaged records. It should be stressed that with this technique, there is some uncertainty as to the exact value of the hair cell potential during current injection. Measurements were considered to be most reliable for hair cells with low characteristic frequencies (< 150 Hz) for which there was the largest difference between the time constant of the recording system and that of the cell membrane. This requirement was met in determinations of reversal potentials by purposely selecting low frequency hair cells for making such measurements.

All data during an experiment were stored on an F.M. tape recorder (band width 0–5 kHz) for subsequent digitization and analysis on a PDP 11/34 laboratory computer. Owing to the presence of considerable narrow band noise in the hair cell membrane potential (Crawford & Fettiplace, 1980) we usually averaged the responses to multiple presentations of tone bursts or efferent shocks. The results to be presented were derived from recordings from seventy-five hair cells which had characteristic frequencies (53–482 Hz), maximum receptor potentials (20–50 mV) and resting potentials (–37 to –65 mV) comparable to those reported before (Crawford & Fettiplace, 1980). All experiments were performed at room temperature (22–25 °C).

#### *Analysis of the response to single efferent shocks*

The responses to single efferent shocks could be classed as failures or successes depending on whether any post-synaptic response was observed. The classification procedure was aided by prior filtering of the records with an 8-pole Butterworth low-pass filter set to a corner frequency which was about half the characteristic frequency of the cell. Such filtering removed the narrow-band fluctuations in the hair cell membrane potential without significantly attenuating the post-synaptic potentials. These were usually large compared to any residual voltage noise, and so there was rarely ambiguity in distinguishing the failures (see Fig. 2). Amplitude histograms of the successes were constructed from unfiltered records by a least-squares method (Baylor, Lamb & Yau, 1979), which involved scaling the ensemble average to produce a least-squares fit to each individual response. The required amplitude was the product of the scaling factor and the amplitude of the average response. In most cases, the scaled means provided a good fit for the individual responses: the correlation coefficients for the fits used in preparing the histograms in Fig. 2B and D had mean values of 0.8 and 0.9 respectively.

#### *Perfusion of the perilymph*

The scala tympani was normally filled with artificial perilymph, which was replenished periodically during the course of an experiment. However, for those experiments in which we wished to vary the composition of the perilymph or to administer drugs, a perfusion system was arranged. The inflow consisted of a fine polythene tube, placed posterior to the otic capsule and gravity fed from a series of reservoirs. The fluid was removed, keeping the level constant by a wick placed in the forebrain cavity. With a flow rate of 150  $\mu$ l/min the fluid in the scala tympani was exchanged several times each minute and although this provided good mixing, the response to changes in composition usually required a few minutes to reach a steady state. The perfusion of the half-head

did not alter the mechanical stability of intracellular recordings, but the turbulent flow did introduce some extra noise into the records. The composition of the standard artificial perilymph was (in mM): NaCl, 130; KCl, 4; CaCl<sub>2</sub>, 2.8; MgCl<sub>2</sub>, 2.2; glucose, 8.0; Na HEPES buffer, 5.0, pH 7.6. The potassium concentration was reduced to 2 mM or elevated to 10 mM at the expense of sodium and changes in chloride concentration were achieved by replacing NaCl with Na methylsulphate

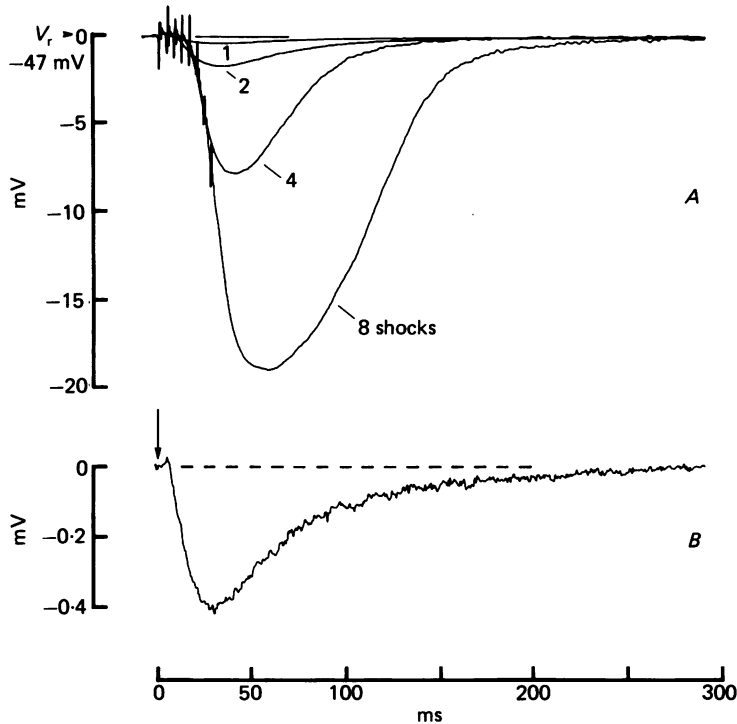


Fig. 1. Average i.p.s.p.s recorded in a hair cell for trains of efferent stimuli comprising different numbers of shocks. *A*, superimposed averages for one, two, four and eight efferent shocks (shock number indicated beside each trace) with records aligned so that first stimulus in each train is coincident. Timing of shocks indicated by capacitive artifacts, intershock interval 4 ms, repetition rate 2/s. Note that each doubling of the shock number produced more than a 2-fold increase in i.p.s.p. size. *B*, single shock response at a higher gain; the shock artifacts have been removed by digitally subtracting the average of the failures, and the timing of the shock is shown by the arrow. Ordinates are membrane potentials relative to resting potential ( $V_r$ ,  $-47$  mV). Number of responses averaged were: 1, 999; 2, 999; 4, 129; 8, 39. Hair cell characteristic frequency 325 Hz; temp.  $24.5$  °C.

(Hopkin & Williams). All cholinergic drugs were purchased from Sigma. In pharmacological and ionic exchange experiments, the measurements on each hair cell were taken in the control solution, then in the test solution and finally again in the control if possible.

## RESULTS

### *General description of efferent post-synaptic potential*

Fig. 1 *A* shows the membrane potential changes in a hair cell for trains of stimuli comprising one, two, four and eight shocks to the efferent axons, and the superimposed averages are aligned so that the first shocks are coincident. The average response to

single shocks is reproduced at a higher gain in Fig. 1 *B*. In this and other cells, single efferent stimuli were relatively ineffective, and evoked an average hyperpolarization that had a peak size of less than 2 mV and lasted for 100–150 ms (see Table 1). The size and wave form of such responses were invariant with the strength of the

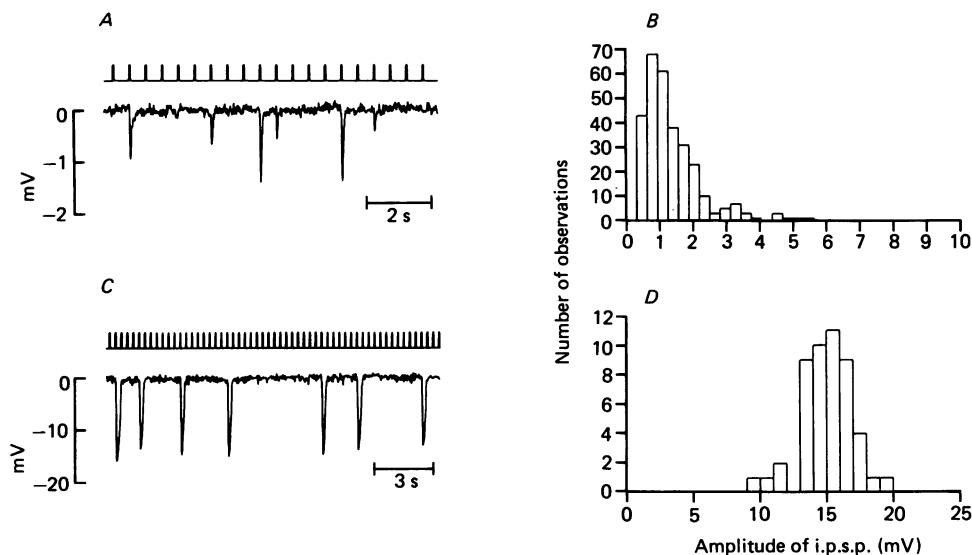


Fig. 2. Left: fluctuations of i.p.s.p.s in two hair cells during repetitive delivery of single efferent shocks; upper trace of each pair shows shock timing (2/s in *A* and 3/s in *C*). Ordinate is membrane potential relative to resting potential and the records have been low-pass filtered with an 8-pole Butterworth filter at 100 Hz (*A*) and 30 Hz (*C*). Resting potentials and characteristic frequencies of cells were: *A*,  $-47$  mV, 325 Hz; *C*,  $-58$  mV, 55 Hz. Note that majority of stimuli failed to evoke a response. Right: histograms of response amplitudes for these two cells. Bin width of histograms, 0.312 mV (*B*) and 1 mV (*D*). Number of trials and failures (not shown in histograms) were: *B* 999, 700; *D* 637, 588.

suprathreshold shocks delivered to the efferent axons. When the number of efferent stimuli was increased, the response was enhanced and a doubling in the shock number caused more than a factor of 2 increase in the size of the hyperpolarization. For example, in Fig. 1, the maximum amplitudes of the average responses to two- and four-shock trains were 1.56 and 7.8 mV respectively, 3.9 times and 19.5 times that to single shocks.

Trains of efferent stimuli containing eight shocks at 4 ms intervals gave close to a maximal hyperpolarization in most cells, and the main effect of additional shocks was a prolongation of the response (see Fig. 12). Post-synaptic potentials resembling those in Fig. 1 were observed in all hair cells studied, and their maximum amplitude ranged between cells from 12 to 30 mV (mean = 17.5 mV,  $n = 54$ ).

#### *Fluctuations with single efferent shocks*

Repeated efferent stimulation with trains containing a small number of shocks generated a hyperpolarization which fluctuated markedly in amplitude, and with

singles or pairs of shocks, a significant fraction of stimuli failed to elicit any response. Examples of the variability are provided in Fig. 2 (left), giving continuous stretches of recordings from different hair cells during repetitive delivery of single shocks. The fraction of stimuli successful was 0.30 based on 1000 presentations (Fig. 2 *A*) and 0.08 from 636 presentations (Fig. 2 *C*). The probability of success depended upon the repetition rate, and increased markedly when the rate was raised above 10/s.

TABLE 1. Properties of i.p.s.p.s produced by single efferent shocks

C.f. (Hz)	$\bar{v}$ (mV)	$f$	$\bar{u}_p$ (mV)	$R$ (s <sup>-1</sup> )
55	1.8	0.08	15	3
103	0.85	0.13	5	2
107	1.50	0.18	9	5
192	0.41	0.07	5	10
200	0.70	0.19	2	2
310	0.19	0.17	1	2
	0.28	0.20	1	3
	0.73	0.42	1	10
325	0.40	0.3	1	2

Data from seven hair cells; c.f. characteristic frequency;  $\bar{v}$ , average peak hyperpolarization;  $f$ , fraction of stimuli that elicited a response;  $\bar{u}_p$ , voltage corresponding to the peak of amplitude histogram, given to the nearest millivolt.  $R$ , repetition rate: note that for one of the cells three different rates are shown. For each cell, measurements were obtained from 500–2000 presentations.

For these two cells, histograms of the i.p.s.p. size, constructed as described in the Methods, are presented in Fig. 2 *B* and *D*. The amplitudes of the majority of responses are grouped around 1 mV for one of the cells and 15 mV for the other. An analysis of the single shock responses was performed on a total of seven hair cells. The peak of the amplitude histogram, or preferred amplitude, was estimated by taking the bin with the largest number of observations and, for each cell, this value is given to the nearest millivolt in Table 1. Despite the dispersion in response sizes for a given cell, it was clear that the preferred amplitude differed between cells (Fig. 2) and there was some suggestion that it was inversely correlated with the cell's characteristic frequency (Table 1). For example, the cells illustrated in Fig. 2 had the lowest and highest characteristic frequencies and their preferred amplitudes were the largest and smallest of the set.

#### *Time course of facilitation*

The results from several cells demonstrated that a pair of efferent shocks was more than twice as effective as a single shock. In Fig. 1 the average response to two shocks separated by 4 ms had an amplitude 3.9 times that to a single shock. Measurements on other cells, gave a value for this ratio of 2.9–6.0 (mean = 4.0,  $n = 5$ , intershock interval 4 ms). The interaction between pairs of shocks was examined in more detail by presenting a test shock at a variable interval following a conditioning shock. Records from such an experiment are given in Fig. 3 *A* which shows the synaptic hyperpolarizations caused by a single stimulus (top trace) and a pair of stimuli separated by 10 ms (middle trace) and 100 ms (bottom trace). These and other records

were obtained by averaging about 200–300 presentations at each interval. They were analysed by computing the facilitation,  $F$  (see Mallart & Martin, 1967).

$$F = \frac{V_2 - V_1}{V_1}, \quad (1)$$

where  $V_1$  and  $V_2$  are the response amplitudes for the conditioning and test shocks respectively. When the interval between shocks was brief so that the individual

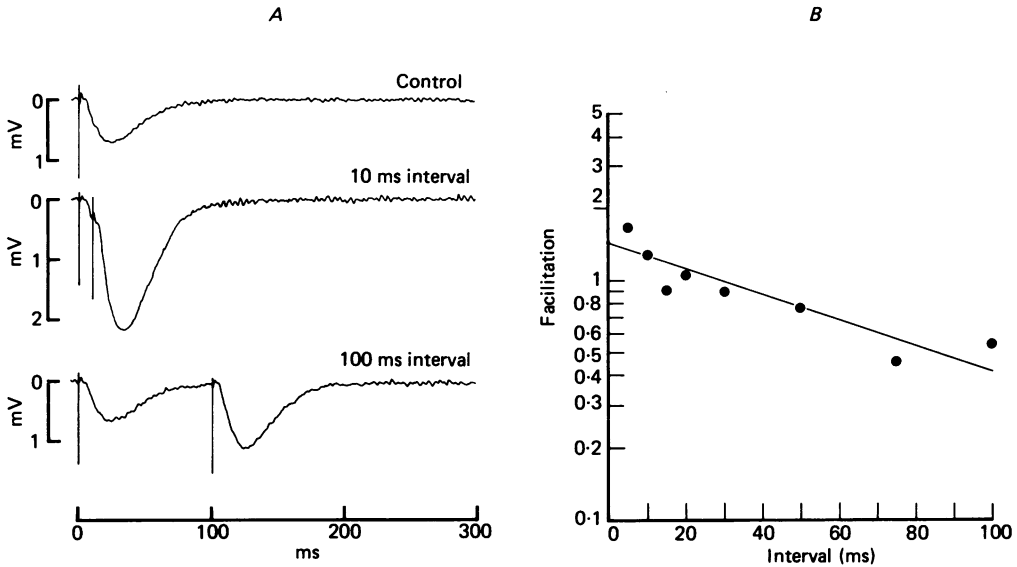


Fig. 3. Decay of facilitation of the response to an efferent test shock following a single conditioning shock. *A*, averaged records for single shocks, and for pairs of shocks separated by 10 and 100 ms; ordinate is voltage relative to the resting potential ( $-47$  mV). *B*, facilitation of response to test stimulus plotted against delay from conditioning stimulus. Ordinate is facilitation ( $F$ ) defined by:  $F = (V_2 - V_1)/V_1$ , where  $V_1$  and  $V_2$  are the average i.p.s.p. sizes for the conditioning and test shocks respectively, measured from records similar to those in *A*. Delay between test shock and next conditioning shock was 500 ms in all cases. Smooth line is least-squares fit corresponding to a time constant of 90 ms.

responses could not be distinguished (as in the middle trace in Fig. 3*A*), the average hyperpolarization to the test stimulus was obtained by first subtracting the control response to the single shock.

Values of  $F$  for this experiment are plotted in Fig. 3*B* and show that the facilitation was prolonged, declining approximately exponentially with shock separation. The line through the points is a least-squares fit corresponding to a time constant of 90 ms. Comparable results, indicating a long-lasting interaction between pairs of stimuli, were obtained in one other cell. This interaction is presumably a major factor contributing to the marked augmentation in i.p.s.p. size for trains of shocks.

*Ionic basis of the efferent post-synaptic response*

In this section, we describe measurements of the membrane conductance changes which underly the efferent post-synaptic potentials, and examine which ionic species might be involved.

*Reversal potential.* Fig. 4*A* shows that the efferent responses were reversed in polarity when the membrane potential was hyperpolarized by injecting long current steps through the intracellular electrode: depolarizing responses were observed for membrane potentials negative to  $-80$  mV. The reversal potential of the slow hyperpolarizing component of the synaptic potential in normal artificial perilymph was determined as  $-79 \pm 5$  mV (mean  $\pm$  s.d.) in nineteen hair cells with an average resting potential of  $-50 \pm 5$  mV. The measurements indicate that the major constituent of the synaptic response arises from an increase in membrane conductance to an ion with an equilibrium potential about 30 mV negative to the resting potential.

Inspection of the records in Fig. 4*A* reveals that there are pronounced differences in the time course of the synaptic response at the various voltage levels. The rate of decay decreases with hyperpolarization from the resting potential and, more conspicuously the delay to the peak of the response shortens at potentials negative to reversal. An explanation previously advanced to account for the latter behaviour is that there are two components to the synaptic response (Art *et al.* 1982); at rest these consist of a small fast depolarization followed by a slower hyperpolarization, with only the later component reversing in the voltage range examined. On this idea, the response at the reversal potential of the slower component should provide an estimate of the time course of the early component alone. For the cell of Fig. 4*A*, we judged that this occurred at a current strength of 0.25 nA, and the efferent response at that level is shown below in Fig. 4*B* after subtraction from the potential change due to the current alone. This record was used as a measure of the time course of the early component, and was then subtracted from the traces in Fig. 4*A* to yield an approximate estimate of the effects of currents on the slower hyperpolarizing component.

The results of the subtraction (Fig. 4*B*) show that this component now reverses in polarity at  $-80$  mV in a manner resembling conventional i.p.s.p.s. Similar subtractions were attempted in other cells, and always produced voltage records more nearly symmetric about the reversal potential. It should be noted that the procedure for separating the two components is an empirical one and has still not totally eliminated the effects of membrane potential on the response wave form, which, in Fig. 4*B*, more than doubled in duration as the cell was hyperpolarized from rest.

We have collected a variety of observations on the early component from different hair cells that establish it to be of synaptic origin. When obtained as described above, it was generally a few millivolts in amplitude, rising during the shock train and lasting for about 30 ms. It could be shown not to be an artifact of capacitive coupling between the stimulating and recording electrodes for it was unaffected by reversing the polarity of the stimulating current. Furthermore, like the slower component, it often fluctuated in amplitude in successive trials, and was abolished by application of curare. Finally, in experiments with single shocks, the mean response was sometimes diphasic and consisted of an initial brief depolarization followed by the slower



hyperpolarization. In such cases, the average of the failures for the hyperpolarizing component gave no hint of any residual depolarization, despite its being evident in the over-all average. These assorted observations suggest that it is of post-synaptic origin and may be produced by the same packets of transmitter responsible for the slower hyperpolarization.

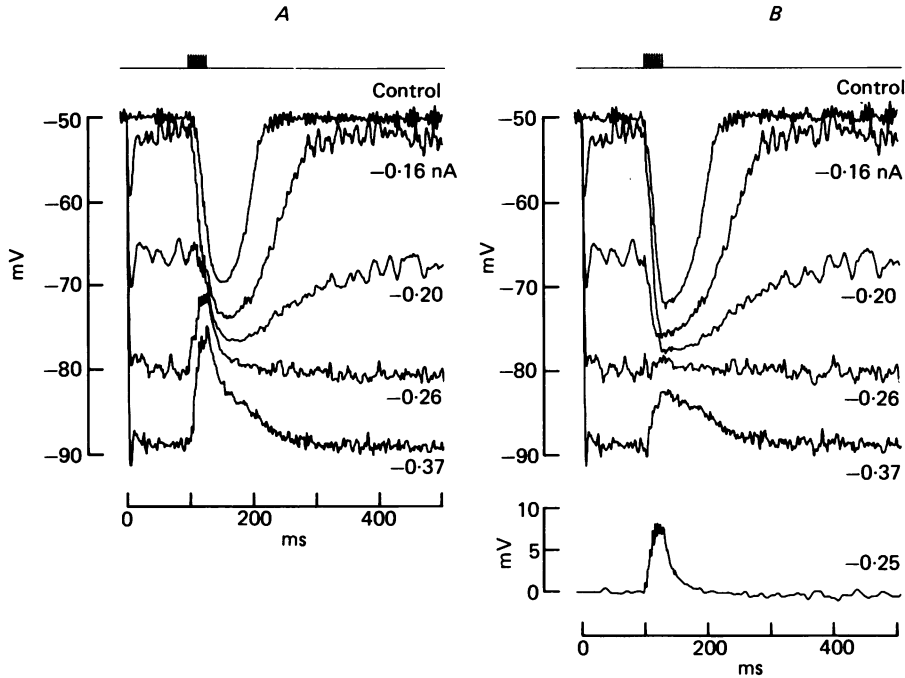


Fig. 4. *A*, effects of steady currents on efferent synaptic potential, demonstrating reversal of polarity. Current pulses begin at time zero, and their strengths in nanoamperes are given beside traces, which are averages of eleven to twenty-six presentations. Efferent shock monitor shown in top trace. Note the change in the time to peak negative to the reversal potential. *B*, average response at  $-80$  mV, shown below, has been subtracted from the records in *A*. Note that the subtracted traces are now more symmetrical about the reversal potential. The response at  $-80$  mV may reflect the time course of an early synaptic component which does not reverse with hyperpolarization; the start and end of the illustrated trace were digitally filtered so as not to add extra noise during subtraction. Hair-cell characteristic frequency, 166 Hz; quality factor of tuning, 6.3.

*Estimates of the synaptic conductance.* Current-voltage curves with and without efferent stimulation are shown in Fig. 5 for the cell of Fig. 4 and one other. The experiments consisted of alternating long current pulses alone (open symbols) with current pulses plus efferent shocks (filled symbols) and all measurements were made at a time corresponding to the peak synaptic hyperpolarization at rest. For almost all cells, the early depolarizing component was virtually complete by this point and will contribute negligibly to the current-voltage relationship. The intersection of the smooth curves through each set of points was used to obtain our best estimate of the reversal potential. Average values for this and other parameters deduced from the

current-voltage relations are listed in Table 2 for the nine hair cells with the largest synaptic hyperpolarizations.

The control current-voltage relationships in Fig. 5 are strikingly non-linear, and are undoubtedly partly shaped by the membrane conductances responsible for

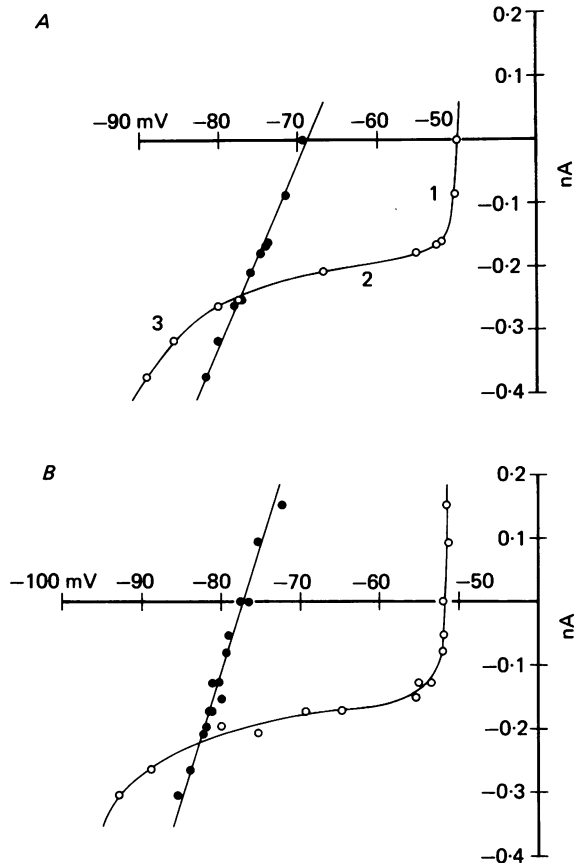


Fig. 5. Steady-state current-voltage curves for two hair cells: open circles, controls; filled circles, during efferent stimulation, measurements taken at a time corresponding to the peak of i.p.s.p. at rest. For each cell the reversal potential of the efferent synaptic conductance was estimated from the intersection of the two curves as: *A*  $-78$  mV; *B*  $-83$  mV. Note that owing to the rectification of the control curves, the slope conductances during efferent stimulation are smaller than the controls at the resting potential. Smooth curves drawn by eye through points. *A* is the same cell as that in Fig. 4.

electrical tuning of the hair cells. To describe their form, we shall divide them into three segments which are of importance for the subsequent discussion: (1) a region of very low resistance, typically less than  $20 \text{ M}\Omega$ , around the resting potential which changed abruptly a few millivolts negative to rest to (2) a high resistance region, greater than  $200 \text{ M}\Omega$ , merging at potentials negative to  $-80$  mV into (3) a secondary decrease in resistance. The sharp transition from low to high resistance regions was seen in a majority of hair cell recordings with the corner about  $2\text{--}10$  mV below the

resting potential. The slope resistances of the two arms of the rectifier (segments 1 and 2) for the cells in Fig. 5 were 10 and 400 M $\Omega$  (Fig. 5A) and 4 and 580 M $\Omega$  (Fig. 5B) and average values from these and other cells are given in Table 2. A similar rectification has been reported for hair cells of the bull-frog *sacculus* (Corey & Hudspeth, 1979).

TABLE 2. Average parameters for current-voltage curves with and without efferent stimulation

Resting potential (mV)	Maximum i.p.s.p. (mV)	Reversal potential (mV)	$R_s$ (M $\Omega$ )	$R_1$ (M $\Omega$ )	$R_2$ (M $\Omega$ )
$-52 \pm 4$	$22 \pm 4$	$-79 \pm 4$	$48 \pm 28$	$18 \pm 25$	$431 \pm 258$

Each number is the mean ( $\pm$ s.d.) of measurements on nine hair cells (characteristic frequencies 71–166 Hz) with maximum i.p.s.p.s of 16–26 mV.  $R_s$ , synaptic resistance at reversal;  $R_1$  and  $R_2$ , slope resistances of control current-voltage curve at the resting potential and about 10 mV hyperpolarized from rest.

In contrast to the control curve, the current-voltage measurements at the peak of the post-synaptic potential are approximately ohmic. To estimate the efferent synaptic resistance, we compared the slope of the line through the efferent measurements with the slope of the tangent to the control curve at the reversal potential. The respective values for the cell of Fig. 5A were 33 and 254 M $\Omega$ . If we regard the synaptic resistance as being inserted in parallel with the resting membrane, we obtain a value for the synaptic resistance of 38 M $\Omega$  at the reversal potential. As might be expected, there was a correlation between the size of the synaptic conductance and that of the synaptic hyperpolarization. A mean value of 21 nS (equivalent to the resistance of 48 M $\Omega$  given in Table 2) was derived from measurements on nine hair cells with maximum synaptic potentials greater than 15 mV.

By comparing measurements made at the same membrane potential (i.e. at reversal) we have demonstrated that efferent stimulation is associated with an increase in the membrane conductance of the hair cell, a conclusion also reached by Flock & Russell (1976) for lateral line hair cells. It is important to point out however that during the course of a large efferent synaptic potential, the membrane potential traverses the most non-linear region of the current-voltage relationship. As a consequence, at the peak of the synaptic potential, there is a net *decrease* in the steady-state conductance relative to that at the resting potential. This is evident in Fig. 5 where the slopes of the control curves around the resting potential are clearly steeper than those for efferent stimulation. Also, compare the mean values in columns 4 and 5 of Table 2. This behaviour can be rationalized in the following manner: as the cell hyperpolarizes due to the activation of the synaptic conductance, other voltage-sensitive conductances are turned off which more than compensate for the increase due to the efferent transmitter channels.

*Ionic species contributing to the synaptic conductance.* Since the efferent transmitter increases the membrane conductance to ions with an equilibrium potential negative to rest, only potassium and chloride ions will be considered as likely current carriers. We have attempted to distinguish between these two candidates by measuring the

reversal potential of the synaptic hyperpolarization during perfusion of the scala tympani with perilymphs of varying ionic composition. The results of an experiment in which the extracellular potassium concentration was raised from its normal 4 mM up to 10 mM are shown in Fig. 6.

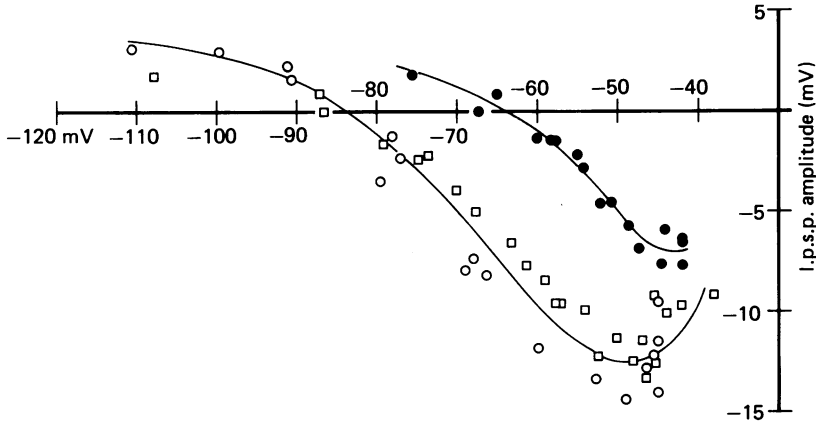


Fig. 6. Effect of changing the extracellular potassium concentration on the reversal of the efferent synaptic potential in a single hair cell. Ordinate is the i.p.s.p. size measured at a fixed time; abscissa, steady membrane potential during the current step. Open circles, 4 mM-potassium; filled circles, 10 mM-potassium; open squares, 4 mM-potassium return control. In this example, the reversal potential was shifted about 20 mV positive on elevation of the perilymphatic potassium concentration. Resting potentials: open circles,  $-45$  mV; filled circles,  $-42$  mV; open squares,  $-44$  mV.

The peak amplitude of the synaptic potential is plotted as a function of the steady membrane potential during the current steps; the filled circles are for high potassium and the open circles and squares are the controls that precede and follow it. The reasonable agreement between the two sets of control measurements testify to the stability of the recording; the smooth curve drawn by eye through the points intersects the abscissa at a reversal potential of  $-84$  mV.

The measurements in high potassium in Fig. 6 are shifted in the depolarizing direction relative to the controls and the new reversal potential is estimated as  $-64$  mV, 20 mV positive to the control value. Measurement from this and two other cells gave a mean positive shift in the reversal potential of  $17 \pm 3$  mV following elevation of the perilymphatic potassium from 4 mM up to 10 mM. For a pure potassium electrode, the expected change in potential would be 23 mV at 25 °C. In another experiment, halving the extracellular potassium concentration caused a negative shift in the reversal potential of 16 mV. These results imply the involvement of potassium ions in the synaptic conductance change.

In Fig. 6, the size of the synaptic potential was not a linear function of the membrane potential, and had a maximum value just negative to the resting potential. This was a common observation (see Fig. 4A) and has also been described for i.p.s.p.s in other cells (Hartzell, Kuffler, Stickgold & Yoshikami, 1977; Horn & Dodd, 1983). There it has been attributed to a voltage sensitivity of the synaptic conductance, but

it may also result partly from the non-linearity of the cell's steady-state current-voltage curve.

In five other experiments we found the reversal potential to be unaltered by a 10-fold reduction in perilymphatic chloride concentration, achieved by its replacement with

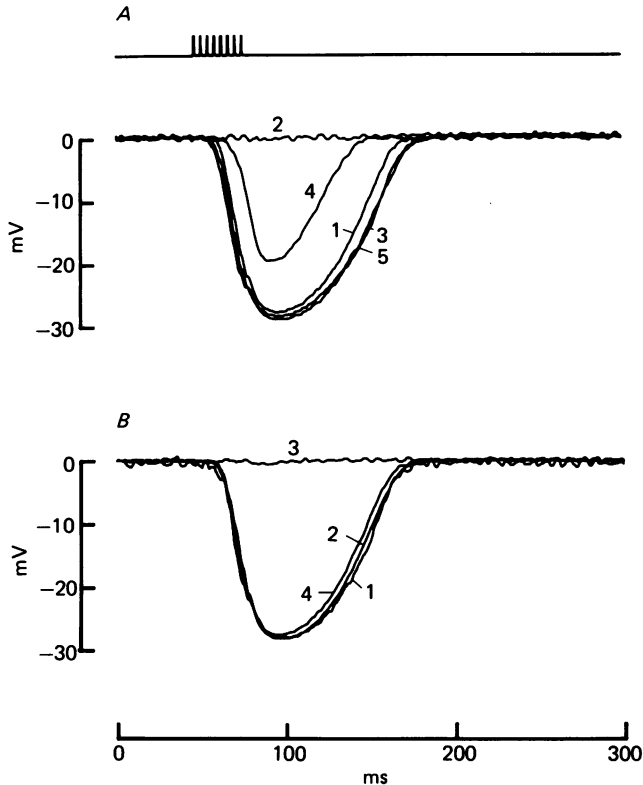


Fig. 7. Block of efferent i.p.s.p. in a hair cell by perfusion with perilymphs containing the cholinergic antagonists *d*-tubocurarine (*A*) and atropine (*B*). The sequence of solution changes is indicated by each set of records, which are averages all obtained from the same hair cell. Ordinates are relative to the resting potential ( $-45$  mV). Between 16 and 152 responses averaged to produce each trace. *A*: 1, control; 2,  $+3$   $\mu$ M-curare; 3, control; 4,  $+0.3$   $\mu$ M-curare; 5, control. *B*: 1, control; 2,  $+0.3$   $\mu$ M-atropine; 3,  $+3$   $\mu$ M-atropine; 4, control.

methylsulphate. For these five different cells the mean reversal potentials before, during and after chloride substitution were  $-81$ ,  $-81$  and  $-77$  mV. In a further experiment, we obtained an apparently normal reversal potential using an intracellular electrode filled with KCl rather than K acetate, a manoeuvre which might have substantially increased the intracellular chloride concentration, considering the small dimensions of the hair cells. Despite an absence of effect on the reversal potential, low chloride substitutions on average halved the maximum size of the synaptic potential at rest. The reason for this is unknown but it may account for an earlier observation by Desmedt & Robertson (1975), that chloride substitutions abolished

effluent inhibition in the mammalian cochlea. Based on this result, the involvement of chloride in the synaptic conductance cannot be entirely eliminated, but it seems likely that potassium ions are the major current carriers.

#### *Cholinergic basis of the efferent synaptic potentials*

Although there is considerable evidence that efferent synaptic action on hair cells of the acousticolateralis system is mediated via the release of acetylcholine (Russell,

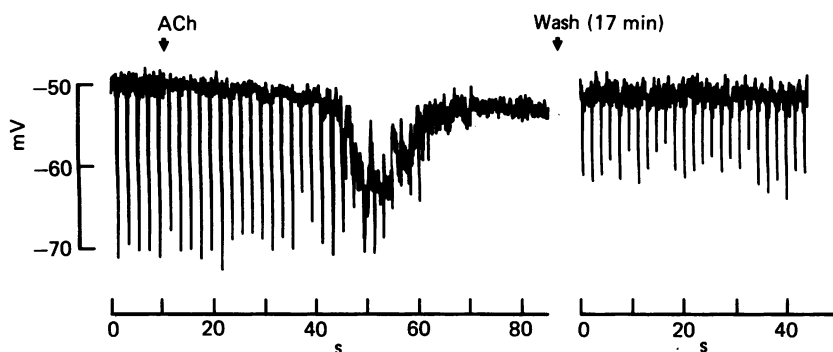


Fig. 8. Effects of acetylcholine (ACh) on the membrane potential and efferent synaptic response in a hair cell. The negative deflexions are i.p.s.s evoked by trains of efferent shocks at 2 s intervals. Scala tympani was continuously perfused with artificial perilymph whose composition at the first arrow was changed to include  $100 \mu\text{M}$ -ACh and  $20 \mu\text{M}$ -neostigmine. The break in the trace at the second arrow denotes a 17 min period of wash with drug-free perilymph. Neostigmine when perfused alone in this and other cells had no effect on the membrane potential.

1971; Guth, Norris & Bobbin, 1976; Robertson & Johnstone, 1978; Klinke, 1981), it is important to confirm the cholinergic nature of the efferent synapse in a preparation where the post-synaptic potentials can be observed directly. The blocking actions of two likely antagonists, curare and atropine are shown in Fig. 7 which gives superimposed averages of the efferent hyperpolarization to eight shocks in the steady states before, during and after perfusion with perilymph containing  $0.3$  and  $3.0 \mu\text{M}$  of each of the drugs. Both antagonists blocked completely and reversibly at the higher concentration, but of the two, curare was slightly more potent causing some reduction in the i.p.s.p. even at the lower concentration. From dose-response curves constructed from measurements in four experiments, the concentrations needed to halve the size of the synaptic potential were estimated as  $0.4 \mu\text{M}$  for curare and  $0.7 \mu\text{M}$  for atropine. Taken at face value, these results indicate that the efferent synapse resembles a peripheral nicotinic synapse such as the neuromuscular junction, since the blocking concentration range for curare is virtually identical in the two systems (Jenkinson, 1970), whereas for atropine it is several orders of magnitude greater than that needed to block a muscarinic receptor (Paton & Rang, 1965). Atropine is about 100 times less potent than curare at the neuromuscular junction (Beránek & Vyskočil, 1968).

A next step in examining the pharmacology would be to infuse a variety of

potential agonists, but the slow rate of administration that we could achieve coupled with a likely desensitization argued against a detailed study. In a few experiments, we perfused with perilymph containing acetylcholine, and an example is illustrated in Fig. 8. This shows a continuous record on a long time scale, broken in the middle during the wash-out period. The downward deflexions of the trace are maximal hyperpolarizations caused by trains of efferent shocks. With a delay after the introduction of a solution containing  $100 \mu\text{M}$ -acetylcholine and  $20 \mu\text{M}$ -neostigmine, there was a transient hyperpolarization followed by an abolition of the responses to efferent axonal stimulation. During this later period, attributed to desensitization of the receptors, it may be noted that there is a small maintained hyperpolarization of the hair cell.

When neostigmine was perfused alone, it never hyperpolarized the cell and had no effect on the time course of the evoked synaptic potential, the duration of which cannot therefore be limited by the breakdown of acetylcholine. However, neostigmine could cause a small (25 %) reduction in the amplitude of the synaptic potential.

Similar effects to those documented above were observed in three other experiments, providing further support for the role of acetylcholine in efferent synaptic transmission.

#### *Inhibition of sound responses at the characteristic frequency*

So far we have been concerned with the events that culminate in the generation of the i.p.s.p.s in the hair cells. Most of the properties observed are shared with slow inhibitory synaptic potentials recorded from other cells (Hartzell *et al.* 1977; Kehoe & Marty, 1980; Hartzell, 1981; Horn & Dodd, 1983). However, the functional significance of inhibition of the hair cells, in contrast to that in many other types of cell, is more obvious particularly since it can be related to inhibition of the cochlear output. In this section we describe the interaction between the synaptic potential and the receptor potential and consider how it might lead to a large desensitization of the auditory nerve fibre responses. We shall be concerned only with acoustic stimulation of the hair cells at their most sensitive or characteristic frequency, where the inhibition was maximal.

*Intensity-amplitude functions.* Fig. 9 shows averaged records from a hair cell that was stimulated with tone bursts of different intensities near its characteristic frequency (221 Hz) and with trains of fourteen shocks to the efferent axons. From control periods before, or well after, the synaptic hyperpolarization, it can be seen that the amplitude of the receptor potential increased with sound pressure, initially in proportion, but then saturating to reach a maximum value of 42 mV peak-to-peak. The existence of the linear region has been documented before (Crawford & Fettiplace, 1980) and it can be illustrated here by noting that the response amplitudes to 40 and 50 dB s.p.l. were 2.2 and 6.6 mV; a factor of 3.16 increase in sound pressure has produced a 3-fold increase in receptor potential.

The shocks to the efferent axons generated a post-synaptic hyperpolarization of 27 mV, throughout the course of which there was a diminution of the receptor potential at all intensities. The amplitude of the control receptor potential (filled circles) and that at the peak of the efferent hyperpolarization (open circles) are plotted as a function of sound pressure in Fig. 10. From the plot, it is clear that the reduction

in the receptor potential at a given sound pressure was largest for low sound pressures producing responses in the linear region, and was reduced at higher levels. Values for the maximum and minimum desensitization in this cell were 8.4 and 1.7 respectively.

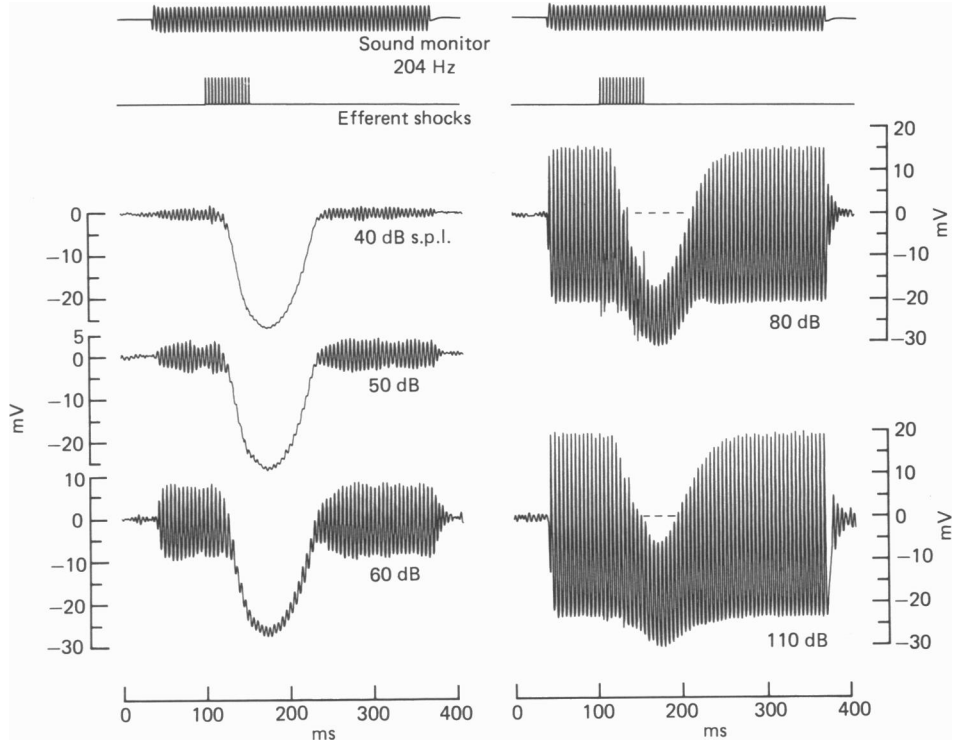


Fig. 9. Efferent inhibition of the receptor potential for tone bursts at 204 Hz close to hair cell's characteristic frequency. Sound pressure of the tone, given in decibels *re*  $20 \mu\text{Pa}$  beside each averaged record increases from the top left to bottom right. Efferents stimulated with trains of fourteen shocks, 4 ms intershock interval. For all traces ordinate gives the membrane potential relative to the resting potential ( $-55 \text{ mV}$ ). Number of responses averaged were: 40 dB, 50; 50 dB, 39; 60 dB, 11; 80 dB, 17; 110 dB, 6. Note the desensitization that occurs throughout the i.p.s.p. Maximum receptor potential, 42 mV; hair cell characteristic frequency, 221 Hz; quality factor of tuning, 4.5. Temp.  $24.7^\circ \text{C}$ .

Measurements on a large number of cells indicated that the maximum or linear desensitization varied considerably from a factor of 1.6 to 28 (mean = 5.3,  $n = 24$ ). The variability is evident in the results collected in Table 3 from ten hair cells, which were selected for the large size of their maximum receptor potentials, and were so judged to be our best recordings. The variation in the amount of inhibition was related to that of the initial sharpness of tuning of the receptor potential, and, as may be seen by comparing columns 4 and 5 in the Table, the largest efferent desensitization in a given cell was roughly proportional to the quality factor ( $Q_{3\text{dB}}$ ) of the cell's control tuning curve. The relation between initial tuning and loss of



sensitivity is expected if the main action of the efferents is to interfere with the hair cell's tuning mechanism.

A corollary is that the inhibition should be more reproducible between cells under circumstances, such as at high sound pressure levels, where their frequency selectivity has deteriorated (Crawford & Fettiplace, 1981*b*). Consistent with this notion is the

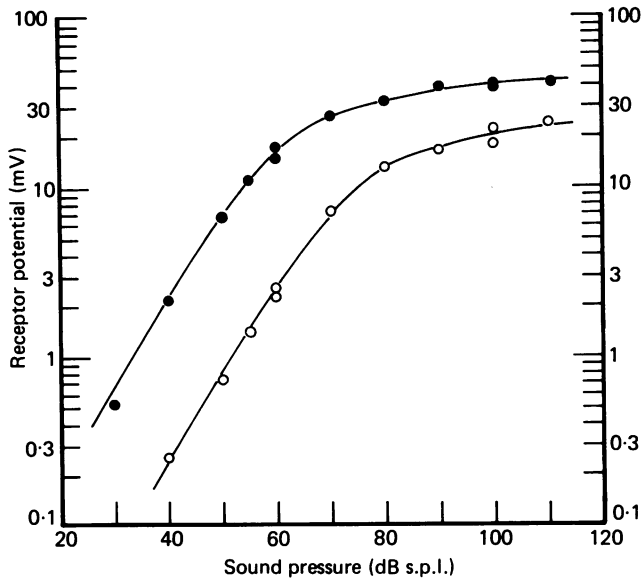


Fig. 10. Intensity-amplitude plots without and with efferent stimulation for the hair cell of Fig. 9. Ordinate is the peak-to-peak amplitude of the receptor potential for tone bursts at 204 Hz, near the hair cell's characteristic frequency. Abscissa, tonal sound pressure in decibels *re* 20  $\mu$ Pa. Measurements were made on records like those in Fig. 9: filled circles, averages of cycles of the receptor potential before and well after the i.p.s.p.; open circles, averages of several cycles at the peak of the efferent hyperpolarization. The smooth curve was drawn by eye through the control points and then displaced down and to the right to best fit the points during efferent stimulation.

observation that the minimum desensitization, inferred from measurements on the saturated parts of the intensity-amplitude curves, varied little, and for those cells in Table 3 ranged from 1.6 to 2.2 (mean = 1.8).

The synaptic hyperpolarization was also a potent suppressor of the spontaneous membrane potential fluctuations which occur in the absence of acoustic stimulation. The fluctuations are narrow-band, with frequency components centred around the cell's characteristic frequency (Crawford & Fettiplace, 1980). An example of the phenomenon is illustrated in the traces in Fig. 4*A*, which were obtained from only small numbers of averages. Vestiges of the voltage fluctuations are visible at the beginning and end of the control record, as well as those superimposed on 0.16 and 0.20 nA currents and in all three records the voltage fluctuations are suppressed throughout the course of the synaptic potential. Abolition of the narrow-band fluctuations is consistent with the efferent desensitization of tone responses at the hair cell's characteristic frequency.

*Relationship to inhibition of afferent fibre responses.* To relate events in the hair cell to inhibition of auditory nerve fibre responses, we shall postulate that each nerve fibre collects from one or a few hair cells tuned to similar characteristic frequencies, and that its excitation is regulated by the absolute membrane potential of the hair cell.

TABLE 3. Summary of efferent inhibition in hair cells

C.f. (Hz)	$R_{\max}$ (mV)	Maximum		Linear desensitization	Sound pressure for 1 mV c.f. response (dB s.p.l.)	Effective afferent inhibition (dB)
		i.p.s.p. (mV)	$Q_{3dB}$			
130	27	17	1.1	3.5	42	66
138*	37	13	2.0	4.6	46	55
138	39	16	3.0	3.6	40	55
200	50	15	6.4	8.9	33	62
221†	42	27	4.5	8.4	34	> 76
242	34	18	5.7	6.7	53	—
331	31	12	6.4	5.1	40	52
346	38	18	8.3	11.8	40	66
353	28	22	9.4	9.8	40	—
481	35	19	5.0	2.8	37	> 74

C.f., characteristic frequency;  $R_{\max}$ , maximum receptor potential at c.f.; i.p.s.p., maximum synaptic potential, obtained with eight efferent shocks except \*, twelve shocks and †, fourteen shocks;  $Q_{3dB}$ , quality factor of linear tuning curve; linear desensitization is maximum reduction in receptor potential at c.f. Effective afferent inhibition is the difference between the sound pressure in column 6 and that producing a receptor potential which depolarized the hair cell 0.5 mV positive to its resting potential at the peak of the i.p.s.p.

This is equivalent to assuming that the release of excitatory transmitter onto the afferent terminals is controlled solely by presynaptic voltage, an assumption for which there is ample evidence in other cells (Katz & Miledi, 1967; Llinás, Steinberg & Walton, 1981).

During the efferent synaptic hyperpolarization, there would have been a reduction in transmitter release, and to achieve the same afferent excitation that existed in the absence of efferent stimulation, it would have been necessary for the receptor potential to depolarize the hair cell positive to the resting potential. It is clear from Fig. 9 that this was not accomplished even at the highest sound pressure of 110 dB s.p.l. Since at this level the receptor potential was virtually saturated, we would conclude that auditory nerve fibres connected to the output of this hair cell would be inhibited at all sound pressure levels.

To quantify the extent of inhibition we may note that the auditory nerve fibre threshold is approximately equivalent to the sound pressure required to generate a characteristic frequency response of about 1 mV in the hair cell (Crawford & Fettiplace, 1980). Extra confirmation of this point is found in Table 3, where the sound pressures needed to produce 1 mV in each cell span the range 33–53 dB s.p.l. which is comparable to recent estimates of the best afferent fibre thresholds in the turtle isolated half-head preparation (see Fig. 1. of Art & Fettiplace, 1984). The effective inhibition can therefore be defined as the difference between the sound

pressure which produced a control receptor potential of 1 mV peak-to-peak, and that producing a receptor potential which at the peak of the i.p.s.p. depolarized the cell to the same level as the control, i.e. 0.5 mV positive to the resting potential. The cell of Fig. 9 produced a control 1 mV response at 34 dB s.p.l., but during the synaptic

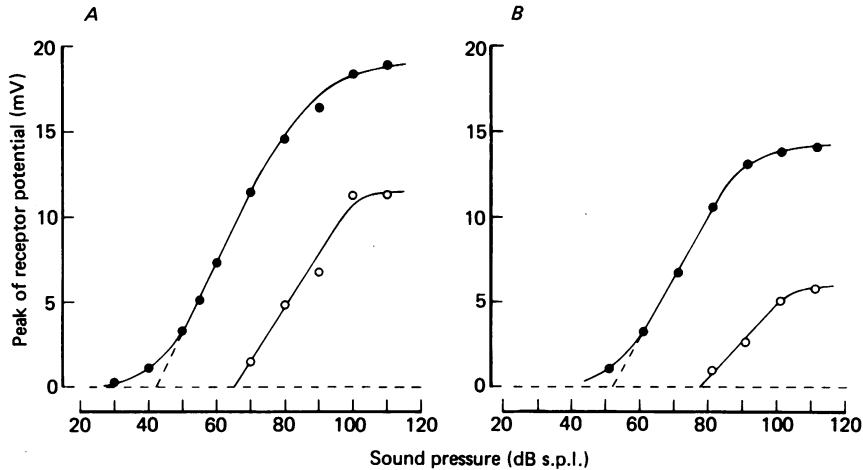


Fig. 11. Peak depolarization of the receptor potential with (open circles) and without (filled circles) efferent stimulation for two different hair cells. Ordinate is the difference between the original resting potential and the membrane potential on the depolarizing phase of the responses to tone bursts; measurements before or during small efferent i.p.s.p.s., the latter being shown only for values positive to the resting potential. For each set of points, the steepest region has been fitted by eye with a straight line and the remainder of the curves are arbitrary. Compare with Fig. 4*B*, Art & Fettiplace (1984). Resting potential and i.p.s.p. size were: *A*,  $-55$  mV,  $3.5$  mV; *B*,  $-50$  mV,  $9.5$  mV.

potential, its membrane potential on the peaks of the sound responses remained negative to the resting potential at 110 dB s.p.l. Therefore the threshold elevation in a corresponding auditory nerve fibre at its characteristic frequency must have been greater than 76 dB. This value compares favourably with the maximum threshold elevation due to the efferents of up to 80 dB seen in turtle auditory afferent axons (Art & Fettiplace, 1984). Similar calculations of the effective nerve fibre inhibition are documented for other hair cells in Table 3; the values obtained range from 52 to greater than 76 dB, equivalent to an elevation in threshold of a factor of between 400 and more than 6300.

Fig. 11 shows intensity–response measurements presented somewhat differently so as to allow a comparison between the hair cell and afferent fibre data over a range of sound pressures. The peak depolarization of the receptor potential, which should determine the amount of transmitter released onto the afferents, is plotted against sound pressure for the conditions with and without efferent stimulation. In each case, it was necessary to use submaximal i.p.s.p.s (3.5 and 9.5 mV for Fig. 11*A* and *B* respectively) so that the plots should be comparable to the afferent fibre rate–intensity functions. The latter are presented in Fig. 4*B* of Art & Fettiplace (1984).

For the control curves, the peak of the receptor potential became more depolarized over a sound pressure range of 40–50 dB before attaining a maximum value; the effective dynamic range was therefore more than an order of magnitude greater than observed in the firing rates of the afferent fibres (mean = 23 dB, Art & Fettiplace,

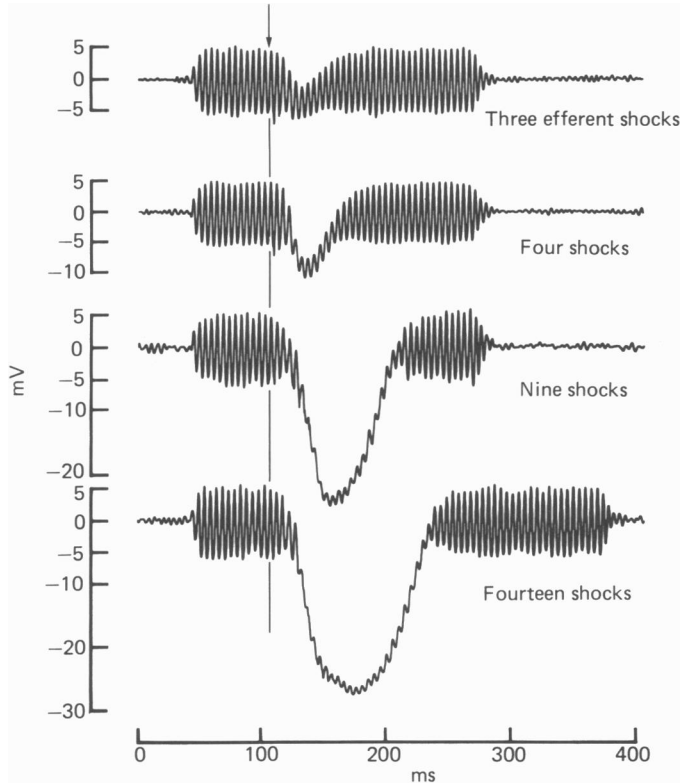


Fig. 12. Inhibition of the receptor potential at a hair cell's characteristic frequency as a function of the number of shocks in the efferent stimulus train. Shock number indicated beside each trace, with timing of first shock shown by arrow. Tone bursts at 204 Hz, 55 dB s.p.l., duration extended for bottom trace. Ordinates are membrane potentials relative to resting potential ( $-55$  mV). Shock number, i.p.s.p. size and maximum desensitization are: 3, 3.2 mV, 2.0; 4, 9.0 mV, 3.3; 9, 24.3 mV, 5.7; 14, 26.9 mV, 7.5. Same cell as Fig. 9. Records are averages of 25–125 presentations.

1984). One reason for the discrepancy might be that the dynamic range of the afferent fibres is truncated by an additional saturation either in the release or post-synaptic action of the transmitter. The changes in the relationship between peak depolarization and sound pressure that occurred during efferent stimulation were qualitatively similar to those seen in the afferent rate–intensity functions. In particular, the function was shifted to higher sound pressures, with a reduction in the saturated level of the depolarization (Fig. 11). There was also some suggestion that the maximum slope of the function was reduced in the presence of efferent stimulation, but this aspect is less pronounced than in the afferent rate–intensity plots.

*Effects of shock number.* The strength of inhibition of the auditory nerve fibre responses can be graded with the number of efferent shocks. Fig. 12 shows the average responses for the hair cell of Fig. 9 to characteristic frequency tones plus trains of efferent stimuli containing three, four, nine and fourteen shocks. The mean synaptic

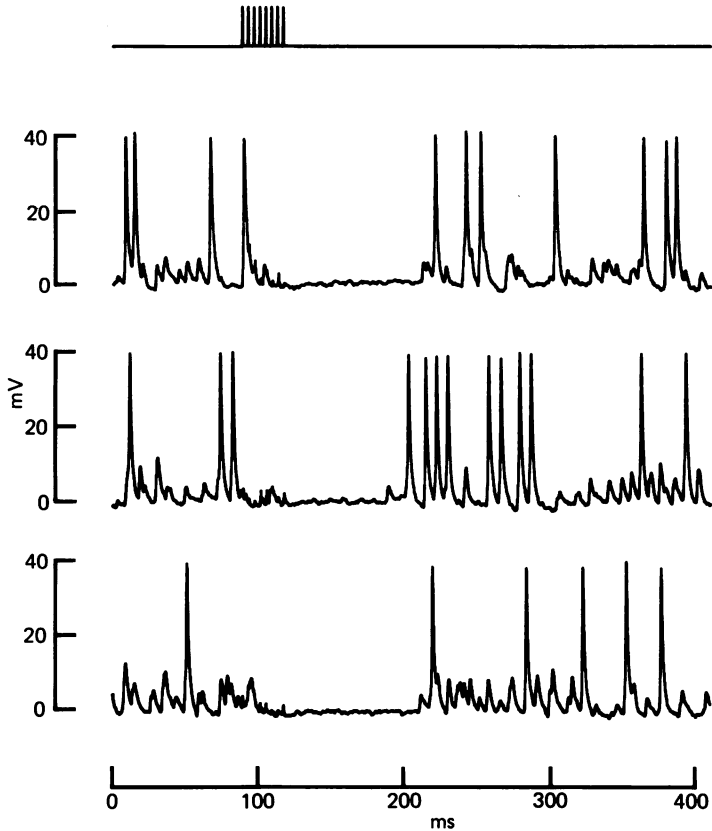


Fig. 13. Intracellular records from an afferent nerve terminal showing inhibition of spontaneous activity following a train of eight efferent shocks whose timing is given in the top trace. Ordinate is membrane potential relative to resting potential ( $-65$  mV). Characteristic frequency of cell, 168 Hz.

potential varied from 3.0 mV for the three-shock train to 27 mV for the fourteen-shock train, and was accompanied by a parallel gradation in the amount of desensitization. At the one extreme, the halving of the receptor potential produced by three shocks scarcely took the membrane potential below rest, but we can estimate, using the same method described above that this corresponds to about a 20 dB threshold elevation in connected afferent fibres. At the other extreme, the size of the synaptic hyperpolarization was comparable for nine and fourteen shocks, and as already calculated, would have resulted in an afferent threshold elevation of greater than 76 dB. Thus the effective threshold elevation deduced in this way is graded over the same range

and occurs with a comparable number of shocks as in direct measurements of efferent inhibition of auditory nerve fibres (Art & Fettiplace, 1984).

#### *Afferent terminal recordings*

The results of analysing the efferent hyperpolarization and sensitivity of the hair cells has led us to the conclusion that most of the afferent fibre inhibition can be accounted for solely by the effects on the hair cells. In a number of experiments, we successfully impaled afferent terminals which allowed us to search for additional signs of efferent synaptic activity. Three consecutive traces from such a recording are presented in Fig. 13. The recording was made in the absence of acoustic stimulation, and illustrates the extensive spontaneous synaptic activity, occasionally triggering impulses, which is presumably driven by the fluctuations in hair cell membrane potential. Following a train of eight efferent shocks, whose timing is illustrated in the top trace, there was a silencing of all activity with no detectable hyperpolarization of the membrane potential. A similar observation has been made by Furukawa (1981) from intracellular recordings from goldfish saccular afferents during efferent stimulation. No obvious hyperpolarization was evident in any of our afferent terminal recordings, which supports the view that efferent inhibition of the turtle cochlea can be largely explained by the effects on the hair cells.

#### DISCUSSION

We have shown that electrical stimulation of the efferent axons to the turtle cochlea evokes in the hair cells large hyperpolarizing synaptic potentials and a concomitant reduction in sensitivity to characteristic frequency tones. The combination of these two effects may be sufficient to account for an elevation in acoustic threshold of close to four orders of magnitude in the afferent axons. The argument applied assumes that a single afferent fibre collects from only a small subset of hair cells tuned to similar characteristic frequencies, a reasonable assumption considering the sharp tuning of the afferent fibres. Although we have no detailed evidence about the pattern of innervation of the basilar papilla, preliminary observations on cochlear whole-mounts stained with Methylene Blue reinforce this assumption. In such whole-mount preparations, each afferent fibre was observed to trace a path directly out across the basilar papilla beneath a single row of about eight hair cells, and fibres were rarely seen to divide and send branches along the papilla.

#### *Synaptic conductance and desensitization*

The conclusion from the reversal experiments is that the slow synaptic hyperpolarization is associated with an increase in the potassium conductance of the hair cell membrane. In the following analysis, we shall postulate that the reduction of hair cell sensitivity is solely a consequence of this synaptic conductance. The desensitization was roughly contemporaneous with the hyperpolarization, which should reflect the time course of the synaptic conductance, since, for the majority of hair cells, it was slow compared to the time constant of the cell membrane.

An equivalent electrical circuit for the hair cell is shown in Fig. 14*A* and will be used to estimate the efferent desensitization at the characteristic frequency for both

low and high sound levels. The circuit comprises three limbs: (1) a transducer conductance which can be modulated about a fixed level  $g_0$ , with a reversal potential at 0 mV (Crawford & Fettiplace, 1981*b*); (2) a frequency-dependent impedance  $Z_r(f)$ , associated with the hair cells resonant properties and in series with a resting potential battery,  $E_r$ ; (3) a synaptic resistance  $R_s$ , with a reversal potential  $E_s$ , which can be switched in by efferent stimulation. We shall assume that the value of  $Z_r(f)$  at the characteristic frequency ( $f_0$ ) of the hair cell can be approximated by the impedance of the parallel resonance used previously to describe the hair cell's tuning (Crawford & Fettiplace, 1981*a*). It can then be related to the steady-state input resistance  $R_i$  by

$$Z_r(f_0) = Q(1 + Q^2)^{\frac{1}{2}} \cdot R_i, \quad (2)$$

where the quality factor,  $Q$ , is a measure of the sharpness of tuning of the resonance (Crawford & Fettiplace, 1981*a*). For the cell of Fig. 5*A*, which had a  $Q$  of 6.3 and an input resistance of 10 M $\Omega$ ,  $Z_r(f_0)$  is about 400 M $\Omega$ . The other circuit parameters are taken from measurements for the cell of Fig. 5*A* ( $E_r = -50$  mV,  $E_s = -78$  mV,  $R_s = 38$  M $\Omega$ ) and from previous data ( $g_0 = 5 \times 10^{-10}$  S, Crawford & Fettiplace, 1981*b*). The linear desensitization,  $S_1$ , was calculated from the reduced equivalent circuit (Fig. 14*B*) as:

$$S_1 = \frac{ER}{E'R'} \left\{ \frac{1 + g_0 R'}{1 + g_0 R} \right\}^2, \quad (3)$$

where  $R$  and  $E$  are the resting resistance and battery and  $R'$  and  $E'$  are the Thevenin equivalents for the combination of resting and synaptic limbs.

The desensitization,  $S_2$ , at loud sound levels was obtained by allowing the transducer conductance to vary between zero and a maximum of  $\bar{g}$  (taken as  $10^{-8}$  S), and can be related to the circuit parameters by

$$S_2 = \frac{ER}{E'R'} \left\{ \frac{1 + \bar{g}R'}{1 + \bar{g}R} \right\}. \quad (4)$$

Applying these equations to the cell of Fig. 5*A*, which had a  $Q$  of 6.3 yields a desensitization of 5.5 at low sound levels and 2.1 at high sound levels. If the  $Q$  of the cell is raised to 10, the corresponding values are 8.2 and 2.2 respectively. In agreement with the experimental results, these calculations demonstrate that the small signal desensitization increases with  $Q$ , whereas the high level desensitization remains approximately constant at around 2.0 (see Table 3).

This analysis represents the simplest view of efferent action, in which the synaptic conductance shunts the high impedance,  $Z_r(f_0)$  of the passive membrane at the cell's characteristic frequency.  $Z_r(f_0)$  was assumed to be ohmic and to increase with  $Q$ , so that the same synaptic conductance would cause a greater desensitization, the larger the value of  $Q$ . It should be noted that this simple analysis will not explain the effects at frequencies well below the characteristic frequency, where efferent stimulation has been found to augment the receptor potential (Art *et al.* 1982). This behaviour is probably a consequence of the fact that, at the peak of the synaptic potential, there is a net *decrease* in the *steady-state* conductance relative to the resting potential, arising because the passive membrane conductance is strongly voltage sensitive and decreases with hyperpolarization.

*Facilitation*

Single shocks delivered at a low repetition rate to the efferent axons generated small and infrequent responses, but with a train of shocks, the synaptic potentials grew in a manner that could not be explained simply by summation of individual events. The large proportion of failures for isolated stimuli could be due either to premature block of the action potential before it invades the efferent terminals, or to its failure

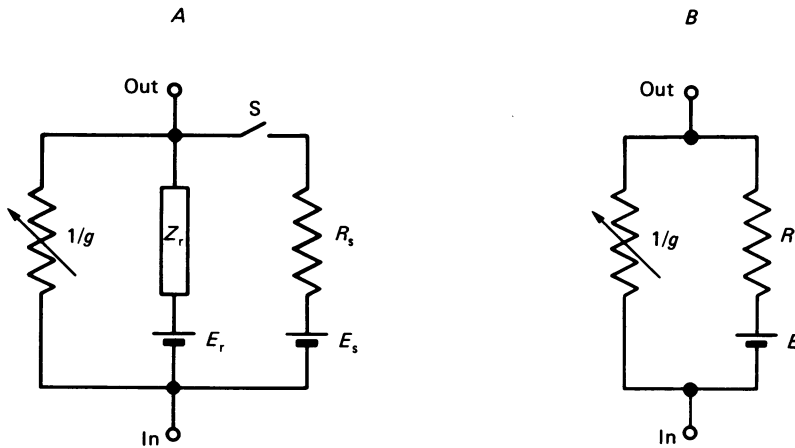


Fig. 14. Equivalent electrical circuit of a hair cell used to calculate the efferent inhibition of the receptor potential at the cell's characteristic frequency. *A*, full circuit:  $g$  is transducer conductance assumed to have a reversal potential of 0 mV and to be modulated by sound about a resting value of  $g_0$  up to a maximum of  $\bar{g}_0$ .  $Z_r$ , frequency-dependent impedance of passive membrane in series with battery  $E_r$ .  $R_s$ ,  $E_s$ , synaptic resistance and battery which are switched in by efferent stimulation. *B*, reduced circuit, with resting and synaptic limbs combined into a single resistance and battery whose values at the hair cell's characteristic frequency are  $R$  and  $E$  with switch,  $S$ , open and  $R'$  and  $E'$  with switch closed.

to release transmitter. However at higher stimulation frequencies, conduction block at branch points would be exacerbated (Grossman, Parnas & Spira, 1979) predicting a greater fraction of failures and smaller average response. The increase in probability and size of response that is actually observed under such conditions therefore seems most likely to be due to an increase in the amount of transmitter released by each action potential that does reach the terminals. The magnitude and time course of this facilitation (Fig. 3) are similar to those described for the frog neuromuscular junction under conditions where the mean quantal content has been lowered by altering the divalent cation concentrations (Mallart & Martin, 1967; Magleby, 1973). The efferent synapse may therefore resemble a neuromuscular junction bathed in low calcium Ringer. The low probability of release to a single stimulus could be important as a protective device to ensure that the tuning and sensitivity of the hair cells are not degraded unnecessarily by spontaneous impulses in the efferent axons.



*Two components of the synaptic response*

The post-synaptic potentials recorded in the hair cell are complex and probably consist of two components, a small early depolarization and a much larger slower hyperpolarization, of which the latter has a time course comparable to the modulation of hair cell sensitivity. The early component was presumably small at the resting potential, and was revealed only by shifting the membrane potential into the high-resistance region of the current-voltage curve. Several observations indicated that it was of synaptic origin and may be mediated by the same packets of transmitter responsible for the slower hyperpolarization. The complexity of the synaptic potential is reminiscent of that seen in amphibian parasympathetic neurones, where the two components have been identified as being due to a nicotinic excitatory and a muscarinic inhibitory input (Hartzell *et al.* 1977). Although two types of cholinergic receptor may coexist on the hair cell, it is conceivable that the early depolarization is the primary synaptic response and itself triggers a sequence of events in the hair cell that culminate in the slower hyperpolarization. Further experiments are needed to settle this point.

This research was supported by a grant from the Medical Research Council, an NIH fellowship to J. J. A., NATO and Wellcome Trust fellowships to P. A. F., and a Howe Royal Society Research fellowship to R. F. We thank Andrew Crawford for many helpful suggestions during the course of the work, and are grateful to Drs P. D. Evans, P. A. McNaughton, B. J. Nunn and M. V. Siegler for commenting on the manuscript.

## REFERENCES

- ART, J. J., CRAWFORD, A. C., FETTIPLACE, R. & FUCHS, P. A. (1982). Efferent regulation of hair cells in the turtle cochlea. *Proceedings of the Royal Society B* **216**, 377-384.
- ART, J. J., CRAWFORD, A. C., FETTIPLACE, R. & FUCHS, P. A. (1983). The ionic basis of efferent synaptic potentials in turtle cochlear hair cells. *Journal of Physiology* **343**, 25-26P.
- ART, J. J. & FETTIPLACE, R. (1984). Efferent desensitization of auditory nerve fibre responses in the cochlea of the turtle *Pseudemys scripta elegans*. *Journal of Physiology* **356**, 507-523.
- ASHMORE, J. F. & RUSSELL, I. J. (1982). Effect of efferent nerve stimulation on hair cells of frog sacculus. *Journal of Physiology* **329**, 25-26P.
- BAYLOR, D. A., LAMB, T. D. & YAU, K. W. (1979). Responses of retinal rods to single photons. *Journal of Physiology* **288**, 613-634.
- BERÁNEK, R. & VYSKOČIL, F. (1968). The effect of atropine on the frog sartorius neuromuscular junction. *Journal of Physiology* **195**, 493-503.
- COREY, D. P. & HUDSPETH, A. J. (1979). Ionic basis of the receptor potential in a vertebrate hair cell. *Nature* **281**, 675-677.
- CRAWFORD, A. C. & FETTIPLACE, R. (1980). The frequency selectivity of auditory nerve fibres and hair cells in the cochlea of the turtle. *Journal of Physiology* **306**, 79-125.
- CRAWFORD, A. C. & FETTIPLACE, R. (1981*a*). An electrical tuning mechanism in turtle cochlear hair cells. *Journal of Physiology* **312**, 377-412.
- CRAWFORD, A. C. & FETTIPLACE, R. (1981*b*). Non-linearities in the responses of turtle hair cells. *Journal of Physiology* **315**, 317-338.
- DESMEDT, J. E. & ROBERTSON, D. (1975). Ionic mechanism of the efferent olivo-cochlear inhibition studied by cochlear perfusion in the cat. *Journal of Physiology* **247**, 407-428.
- FLOCK, Å. & RUSSELL, I. (1976). Inhibition by efferent nerve fibres: action on hair cells and afferent synaptic transmission in the lateral line canal organ of the burbot *Lota lota*. *Journal of Physiology* **257**, 45-62.

- FURUKAWA, T. (1981). Effects of efferent stimulation on the saccule of goldfish. *Journal of Physiology* **315**, 203-215.
- GROSSMAN, Y., PARNAS, I. & SPIRA, M. E. (1979). Differential conduction block in branches of a bifurcating axon. *Journal of Physiology* **295**, 283-305.
- GUTH, P. S., NORRIS, C. H. & BOBBIN, R. P. (1976). The pharmacology of transmission in the peripheral auditory system. *Pharmacological Reviews* **28**, 95-125.
- HARTZELL, H. C. (1981). Mechanisms of slow postsynaptic potentials. *Nature* **291**, 539-544.
- HARTZELL, H. C., KUFFLER, S. W., STICKGOLD, R. & YOSHIKAMI, D. (1977). Synaptic excitation and inhibition resulting from direct action of acetylcholine on two types of chemoreceptors on individual amphibian parasympathetic neurones. *Journal of Physiology* **271**, 817-846.
- HORN, J. P. & DODD, J. (1983). Inhibitory cholinergic synapses in autonomic ganglia. *Trends in Neuroscience* **6**, 180-184.
- JENKINSON, D. H. (1960). The antagonism between tubocurarine and substances which depolarize the motor end-plate. *Journal of Physiology* **152**, 309-324.
- KATZ, B. & MILEDI, R. (1967). A study of synaptic transmission in the absence of nerve impulses. *Journal of Physiology* **192**, 407-436.
- KEHOE, J. & MARTY, A. (1980). Certain slow synaptic responses: their properties and possible underlying mechanisms. *Annual Review of Biophysics and Bioengineering* **9**, 437-465.
- KLINKE, R. (1981). Neurotransmitters in the cochlea and cochlear nucleus. *Acta oto-laryngologica, Stockholm* **91**, 541-554.
- KLINKE, R. & GALLEY, N. (1974). Efferent innervation of vestibular and auditory receptors. *Physiological Reviews* **54**, 316-357.
- LLINÁS, R., STEINBERG, I. Z. & WALTON, K. (1981). Relationship between presynaptic calcium current and post-synaptic potential in squid giant synapse. *Biophysical Journal* **33**, 323-352.
- MAGLEBY, K. L. (1973). The effect of repetitive stimulation on facilitation of transmitter release at the frog neuromuscular junction. *Journal of Physiology* **234**, 327-352.
- MALLART, A. & MARTIN, A. R. (1967). An analysis of facilitation of transmitter release at the neuromuscular junction of the frog. *Journal of Physiology* **193**, 679-694.
- PATON, W. D. M. & RANG, H. P. (1965). The uptake of atropine and related drugs by intestinal smooth muscle of the guinea-pig in relation to acetylcholine receptors. *Proceedings of the Royal Society B* **163**, 1-44.
- ROBERTSON, D. & JOHNSTONE, B. M. (1978). Efferent transmitter substance in the mammalian cochlea: Single neuron support for acetylcholine. *Hearing Research* **1**, 31-34.
- RUSSELL, I. J. (1971). The pharmacology of efferent synapses in the lateral line system of *Xenopus laevis*. *Journal of Experimental Biology* **54**, 643-658.